

Physical Aging of Poly(diethylene glycol-*p,p'*bibenzoate)

GALINA ZAMFIROVA,^{1*} MARIJKA MISHEVA,² MANIA KRESTEVA,² NIKOLAJ DJOURELOV,²
ROSARIO BENAVENTE,¹ ERNESTO PÉREZ,¹ JOSÉ M. PEREÑA¹

¹ Instituto de Ciencia y Tecnología de Polímeros (CSIC), Juan de la Cierva, 3. 28006 Madrid, Spain

² Sofia University "Kl. Ohridsky," Faculty of Physics, Department of General Physics, James Bourchier Blvd., 5. 1126 Sofia, Bulgaria

Received 5 June 2001; accepted 27 June 2001

ABSTRACT: The structure of a quenched sample of a liquid crystalline polyester, poly(diethylene glycol-*p,p'*-bibenzoate) (PDEB), and its physical aging was studied by microhardness methods (MH), wide-angle X-ray scattering (WAXS), and positron annihilation lifetime spectroscopy (PALS). It was established that the smectic layers in the liquid crystalline domain are oriented parallel to the sample plane. Physical aging leads to an increase of either the Vickers microhardness, directly related to the elastic modulus of the material, or the total microhardness, which includes all the components of the overall deformation. These mechanical changes are due to a decrease in the sizes of nanopores and the consequential increase of the density of the disordered phase.
© 2002 John Wiley & Sons, Inc. *J Appl Polym Sci* 83: 2363–2368, 2002

Key words: poly(diethylene glycol-*p,p'*-bibenzoate); liquid crystal polymers; structural studies; positron annihilation; microhardness

INTRODUCTION

A typical feature for almost all polymers is structural change with time and, therefore, variation of mechanical properties (i.e., polymers age and are materials with time-dependent mechanical properties).

When a polymeric material is quenched from a temperature above its glass transition temperature (T_g) to another below its T_g , the polymer sample is in a nonequilibrium state and the time-

dependent structural change to the equilibrium state is known as physical aging.^{1,2} This process is accompanied by an increase of density in the material and a decrease in the free volume holes. The aging process of amorphous and semicrystalline polymers is relatively well studied.^{1–5} At the same time, there are only a few works concerning physical aging of liquid crystalline polymers.^{6–11}

The aim of this investigation is to study the physical aging of liquid crystalline poly(diethylene glycol-*p,p'*-bibenzoate) (PDEB), of which smectic S_A structure and properties change very fast.⁹ The presence of the central ether group in the spacer inhibits the transition of mesophase into crystal phase, typical for polybibenzoates with only methylene units in the spacers.^{6,10,11} The present study of the physical aging process of PDEB includes its structure and some mechanical properties, as well as their changes during the process.

* Permanent address: Higher Institute of Transport Engineering "T. Kableshev," Geo Milev Str., 158, 1574 Sofia, Bulgaria.

Correspondence to: G. Zamfirova (ictz351@ictp.csic.es).

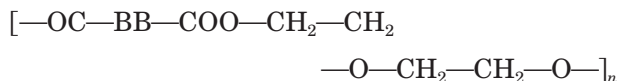
Contract grant sponsor: NATO Science Committee; contract grant sponsor: Bulgarian Academy of Sciences; contract grant sponsor: Spanish Council for Scientific Research; contract grant number: 2001 BG 0003.

Journal of Applied Polymer Science, Vol. 83, 2363–2368 (2002)
© 2002 John Wiley & Sons, Inc.
DOI 10.1002/app.10216

EXPERIMENTAL

Materials

The chemical structure of the polymer under study is



where BB stands for the bibenzoic unit. The method of synthesis is described in ref. 6. The T_g obtained by DSC⁸ is 55°C. The material was molded at 190°C, pressed, and then quenched in ice water. Several portions of this quenched sample were annealed for different times (from 5 to 120 min) at 36°C. After finishing the annealing process, each portion was kept in a container thermostated with ice water to fix the structure. For wide-angle X-ray scattering (WAXS) and microhardness (MH) studies, each portion was maintained for 5 min at room temperature and then measured.

Microhardness Measurements

MH measurements were performed by using loads between 1.25 and 160 g on a microhardness tester, *mhp-160*, attached to a NU-2 microscope. The indenter is a regular square pyramid with a top angle of 136°. From the projected diagonal length of the indentation at either loaded or unloaded state, different MH characteristics can be determined, as follows:

1. Vickers microhardness (MHV). This is a parameter characterizing the material plastic resistance against pyramid penetration. MHV is connected with the irreversible component of deformation. It is calculated according to

$$\text{MHV} = kP/d^2 \quad (1)$$

where k is a constant, deduced from the pyramid geometry, and d is the diagonal of the projected area of indentation after taking out the indenter.

2. Total microhardness (MHT). This characteristic is defined on the analogy of MHV as^{12,13}

$$\text{MHT} = kP/D_2 \quad (2)$$

where D is the diagonal of the indentation in the loaded state. Thus defined, this value can be considered as a measure for the material total resistance against indenter penetration. MHT is connected with the total deformation, including elastic, plastic, and viscoelastic components.

Positron Annihilation Lifetime Spectroscopy (PALS)

PALS is a very useful tool for direct evaluation of the radii of free-volume holes, localized in the disordered regions of polymers. The PAL technique is applicable to pore sizes in the range of the subnanopores (0.2–2 nm). The method is based on the behavior of positrons in the condensed matter. When a positron from a radioactive source, such as ²²Na with mean kinetic energy around 0.21 MeV, enters a solid sample, it rapidly spends up its energy on ionizing and exciting the matrix atoms and becomes thermalized in $\sim 10^{-12}$ s. The thermalized positron can annihilate as a free particle in ~ 150 –300 ps. Because of its positive charge, the positron can be trapped in an open volume before annihilation. Here, because of lower electron density, positron can exist before annihilation for a longer time, which depends on the free-volume size. In molecular solids, positron can form, with a medium electron, a bound system called positronium (Ps). It exists in singlet or triplet state, para-Ps (p-Ps) and ortho-Ps (o-Ps), respectively. Para-Ps self-annihilates in 125 ps, whereas the time of o-Ps self-annihilation in vacuum is ~ 140 ns. In the sample, the o-Ps can pick up one of the surrounding electrons and annihilates it in several nanoseconds, the so-called pick-off process. The o-Ps lifetime, τ , depends on the pore sizes. If an infinite spherical potential of radius R_0 with an electron layer of thickness ΔR is supposed,^{14,15} the relationship between τ and the free-volume hole radius R ($R = R_0 - \Delta R$), is

$$\tau = \frac{1}{\lambda} = 0.5 \left[1 - \frac{R}{R_0} + \frac{1}{2\pi} \sin\left(\frac{2\pi R}{R_0}\right) \right]^{-1} \quad (3)$$

where τ is in nanoseconds and R is in angstroms. The empirically found value of ΔR is 0.1656 nm.¹⁵

The lifetime spectrometer used is a standard fast-fast coincidence apparatus based on ORTEC Electronics. The time resolution was around 280 ps full width at half-maximum. For data processing, the program PATFIT,¹⁶ with which a lifetime spectrum is fitted by a sum of exponentials, was used.

Two consecutive PAL measurements at room temperature were made on the initial nonaged quenched sample, with a time interval of 1 week.

WAXS Measurements

WAXS studies were performed by means of an X-ray diffractometer Siemens D-500 by using Cu $K\alpha$ radiation in transmission and reflection modes.

RESULTS AND DISCUSSION

Microhardness Measurements

Both parameters (MHV and MHT) as a function of loading, for the sample annealed during 120 min at 36°C, are presented in Figure 1. As the loading is greater, the depth of penetration is higher and the microhardness of the inner layers is measured. There is a well-pronounced maximum for MHV at low loads, which means a greater resistance against the plastic deformation of the layers close to the surface. This greater resistance could be a consequence of the quantity or perfection of the more ordered supermolecular structural units, their better arrangement, eventually their parallel orientation to the surface, or a combination of these reasons.

The dependence of MHT versus aging time, measured at 20 g loading, is shown in Figure 2. MHV, measured with a 24 g load and reported in ref. 8, is presented for comparison in the same

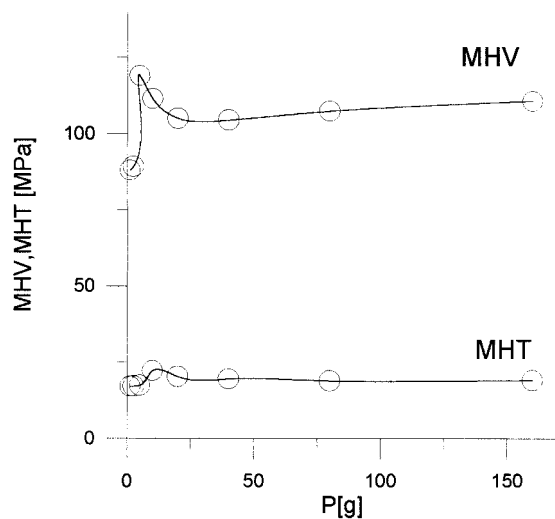


Figure 1 Dependence of microhardness (MHV and MHT) as a function of loading.

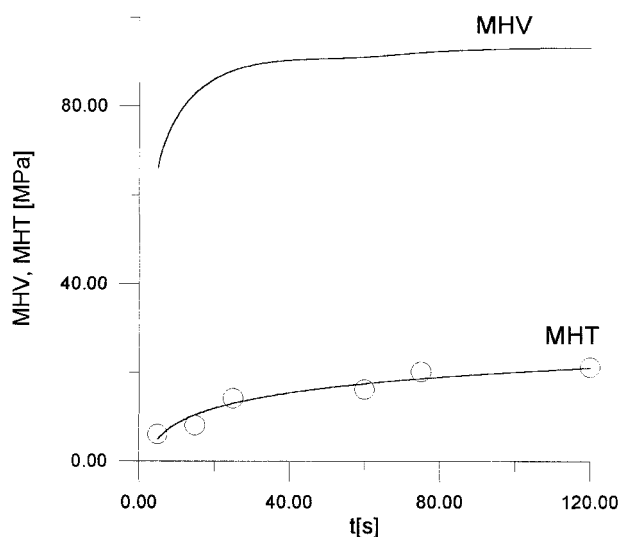


Figure 2 Dependence of microhardness (MHV and MHT) as a function of aging time.

figure. It can be seen that MHV increases predominantly during the first half an hour of aging. Because MHV is sensitive to structures which show resistance to plastic deformation, it can be supposed that in the first 30 min the aging induces a reinforcement of the intermolecular connections, but it cannot be specified which phase, LC or amorphous, is more affected. Therefore, to clarify the structure of the sample and its changes during the aging process, WAXS and PALS investigations were carried out.

WAXS Studies

The X-ray patterns of the samples, annealed for different aging times at 36°C, in reflection and transmission modes, are shown in Figure 3. X-ray patterns measured at reflection consist of a set of narrow reflections overlapping on the amorphous halo [Fig. 3(a)]. This result shows that quenching does not prevent the formation of a quite perfect smectic phase.

The obvious difference between the X-ray patterns obtained in reflection and transmission modes could be explained by the assumption that smectic planes are oriented in the plane of the sample as a result of the pressing process. According to this suggestion, scattering at reflection would be obtained by the smectic layers and amorphous macromolecules but not from the mesogens within the layers. On the other hand, at transmission mode the diffraction from the smectic planes could not be observed, whereas the

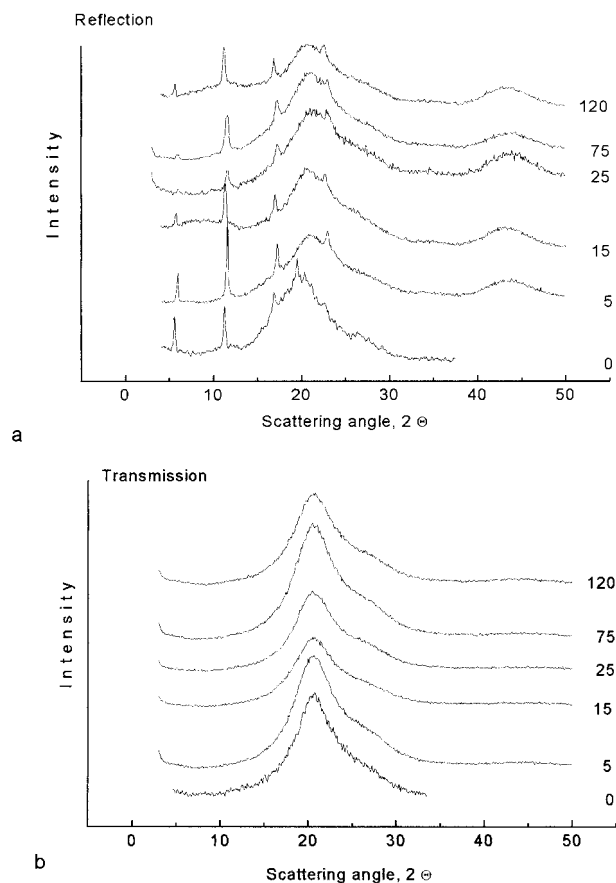


Figure 3 Wide-angle X-ray diffraction patterns of PDEB sample, measured at reflection (a) and transmission (b) modes.

contribution to the amorphous scattering would arise mainly from the distances between molecules within the smectic domains. This result confirms the previous supposition based on the microhardness measurements about orientation of the smectic planes parallel to the sample surface.

Positron Annihilation Lifetime Spectroscopy

Three- and four-term analyses of the lifetime spectra were attempted. The four-term analysis was successful only if the shortest lifetime τ_1 was fixed, and a linear constraint, $I_2 + I_3 = 3 I_1$, of the relative intensities was used. The mean lifetimes, $\tau_m = \sum \tau_n I_n$ ($n = 1-N$, $N = 2, 3$, and 4, respectively), obtained coincided in the error limits. The results from the three- and four-term fits of the time spectra were presented in Table I. The pore radii, calculated by eq. (3), are also given.

As was established by many authors,¹⁷ because of positron irradiation during the time of measurements, the intensity of the o-Ps lifetime decreases for some kinds of polymers. In the present case, four consecutive measurements were made for 24 h and no unidirectional change in the o-Ps intensities was observed. So, the effect of 24-h positron irradiation of PDEB (source activity about 8×10^5 Bq) is negligible.

Following one of the widely accepted interpretations of positron lifetimes in polymers, the two shorter lifetimes, τ_1 and τ_2 , should be ascribed to p-Ps and free (i.e., not formed positronium) positron annihilation.¹⁸ These lifetimes are not

Table I Positron Lifetimes τ_n , Their Relative Intensities I_n , Mean Lifetime τ_m , and Pore Radii R_n from Three- and Four-Component Fit of Positron Lifetime Spectra

First Measurement					Second Measurement				
τ (ps)	I (%)	R (nm)		τ (ps)	I (%)	R (nm)			
Three-Component Fit									
τ_1	301	I_1	72.7	—	τ_1	289	I_1	63	—
τ_2	635	I_2	18.8	—	τ_2	495	I_2	26	—
τ_3	1823	I_3	8.8	0.296	τ_3	1531	I_3	10.4	0.249
τ_m	497				τ_m	473			
τ (ps)	I (%)	R (nm)		τ (ps)	I (%)	R (nm)			
Four-Component Fit (τ_1 -Fixed)									
τ_1	125	I	5.74	—	τ_1	125	I_1	5.1	—
τ_2	377	I_2	77	—	τ_2	337	I_2	79.7	—
τ_3	1030	I_3	12.9	0.172	τ_3	1230	I_3	14.1	0.200
τ_4	2200	I_4	4.3	0.305	τ_4	1700	I_4	0.6	0.260
τ_m	498				τ_m	459			

sensitive to structural changes of a polymer.¹⁹ The two longer lifetimes, τ_3 and τ_4 , should be considered as due to o-Ps pick-off annihilation at free-volume holes and their values depend on pore sizes via eq. (3).

Recently, the physical meaning of the o-Ps intensity is under debate. It was shown²⁰ that the equation²¹

$$F_v = CI_{\text{o-Ps}}V(\tau_{\text{o-Ps}}) \quad (4)$$

where C is a fitting parameter and $V(\tau_{\text{o-Ps}}) = (4/3)\pi R^3$ is the pore size, does not give the correct absolute values of fractional free volume F_v . Equation (4), however, could be used to determine qualitatively the trend in F_v variation when the polymer is subjected to some treatments. In the present case, the temperature, pressure, and chemical composition of the polymer studied were the same between and during the time of measurements. Therefore, the change of parameter $F_r = I_{\text{o-Ps}}V(\tau_{\text{o-Ps}})$ could be considered a measure of the variation of the fractional free volume F_v .

Physical aging of PDEB at room temperature, as it can be seen from Table I, results in a decrease in the longest lifetime and an increase in its intensity, for a three-component fit. This means that dimensions of free-volume holes decrease whereas their quantity increase (i.e., the amorphous phase becomes more homogeneous during aging).

Four-term analysis shows a decrease of both longest lifetime τ_4 and its intensity. Moreover, the value and the relative intensity of the shorter o-Ps lifetime τ_3 slightly increases. Therefore, the four-term analysis clarifies the homogenization of pores, because the difference between the sizes of the pores decreases (i.e., decreases the pore size dispersion). It seems that most of the larger pores collapsed, whereas the remaining (<1%) only diminished their sizes. The parameter P was decreased from 0.78 to 0.51 (i.e., about 34%). These observations are in agreement with the published results on physical aging of polymers^{22,23} and are confirmed by the present results on PDEB, of which rate of density increase is considerable even at room temperature (i.e., well below its T_g).

CONCLUSIONS

The structure of quenched PDEB samples consists of smectic domains and amorphous areas.

The smectic layers in the liquid crystalline domain are oriented parallel to the sample plane.

Physical aging leads to an increase of the total microhardness as well as the Vickers one, related directly to the elastic modulus of the material.

The changes of mechanical properties during the aging process are due to the decrease of the distance between macromolecule segments in amorphous area (i.e., decreasing the sizes of nanopores and increasing the density in the disordered phase).

We thank the NATO Science Committee for the inviting scientist grant awarded to one of us (G.Z.). The support from the CICYT (project MAT98-0961-C01) and from the project 2001BG003 (Bulgarian Academy of Sciences and the Spanish Council for Scientific Research (CSIC)) is also gratefully acknowledged.

REFERENCES

1. Struik, L. C. E. *Physical Aging of Amorphous Polymers and Other Materials*; Elsevier: Amsterdam, 1978.
2. McKenna, G. B. *Glass Formation and Glassy Behavior*; In *Comprehensive Polymer Science*; Both, C. and Price, C., Eds., Pergamon Press: Oxford, U.K., 1989; Vol. 2; p 311.
3. Struik, L. C. E. *Polymer* 1989, 28, 1521–1533; *Polymer* 1987, 30, 799–815.
4. Matsuoka, S. *Relaxation Phenomena in Polymers*; Hanser Publishers: Munich, 1992.
5. Plazek, D. J.; Andreanovic, R. A. *Physical Aging of Amorphous Polymers*; In *Keynote Lectures in Selected Topics of Polymer Science*; Riande, E., Ed., CSIC: Madrid, 1995; Chapter VI.
6. Bello, A.; Pereña, J. M.; Pérez, E.; Benavente, R. *Macromol Symp* 1994, 84, 297–306.
7. Benavente, R.; Pereña, J. M.; Pérez, E.; Bello, A. *Polymer* 1993, 34, 2344–2347.
8. Pérez, E.; Pereña, J. M.; Benavente, R.; Bello, A.; Lorenzo, V. *Polym Bull* 1992, 29, 233–237.
9. Pérez, E.; Benavente, R.; Marugán, M. M.; Bello, A.; Pereña, J. M. *Polym Bull* 1991, 25, 413–418.
10. Pérez, E.; Bello, A.; Marugán, M. M.; Pereña, J. M. *Polym Commun* 1990, 31, 386–387.
11. Pérez, E.; Marugán, M. M.; Wanderhart, D. *Macromolecules* 1993, 26, 5852–5859.
12. Zamfirova, G.; Dimitrova, A. *Polym Testing* 2000, 19, 533–542.
13. Pereña, J.; Lorenzo, V.; Zamfirova, G.; Dimitrova, A. *Polym Testing* 2000, 19, 231–236.
14. Eldrup, M.; Lightbody, D.; Sherrod, J. N. *J Chem Phys* 1981, 63, 5.

15. Nakanishi, H. S.; Wang, J.; Jean, Y. C. *Positron Annihilation Study of Fluids*; Sharma, S. C., Ed., World Scientific: Singapore, 1987.
16. Kirkegaard, P.; Pedersen, N. J.; Eldrup, M. PAT-FIT-88; Risoe National Laboratory: Roskilde, Denmark, 1989.
17. Suzuki, T.; Oki, Y.; Numajiri, M.; Miura, T.; Kondo, K.; Ito, Y. *Positron Positronium Chem.*, 3rd International Workshop, Jean, Y. C., Ed., World Scientific: Singapore, 1990; pp 39–46.
18. Dlubek, G.; Saarinen, K.; Fretwell, H. M. *Nucl Instrum Methods Phys Res Sect B* 1998, 142, 139–155.
19. Xie, L.; Gidley, D.; Hristov, H. A.; Yee, A. F. *Polymer* 1995, 35, 14–17.
20. Schmidt, M.; Maurer, F. H. *J Radiat Phys Chem* 2000, 58, 535–538.
21. Nakanishi, H.; Wang, Y. Y.; Jean, Y. C.; Sandreczki, T. C. *Positron Annihilation in Fluid*; Sharma, S. C., Ed., World Scientific: Singapore, 1988.
22. Wang, B.; He, C. Q.; Zhang, J. M.; Li, S. Q.; Wang, S. J.; Shi, J. Z.; Ma, D. Z. *Phys Lett A* 1997, 235, 557–561.
23. Waslund, C.; Schmidt, M.; Schantz, S.; Maurer, F. H. *J Polym Eng Sci* 1998, 38, 1286–1294.